Construction and Building Materials 112 (2016) 816–824

Contents lists available at ScienceDirect

Construction and Building Materials

journal homepage: www.elsevier.com/locate/conbuildmat

White Ordinary Portland Cement blended with superfine steel dust with high zinc oxide contents

Henry A. Colorado [a,*], Edwin Garcia [b], M.F. Buchely [c]

[a] CCComposites Laboratory, Universidad de Antioquia UdeA, Calle 70 No. 52-21, Medellin, Colombia
[b] Department of Civil Engineering, Universidad de Antioquia, Medellin, Colombia
[c] Mechanical Engineering Department, Universidad de los Andes, CR 1E 19A 40, 111711 Bogota DC, Colombia

ARTICLE INFO

Article history:
Received 15 August 2015
Received in revised form 7 February 2016
Accepted 25 February 2016

Keywords:
Portland cement
Steel dust
Ceramic powders
Composite
Cement paste
Mortar

ABSTRACT

The addition of steel waste in the form of slags and dust to cement is beneficial to the environment because waste can be immobilized, and thus, decreasing the waters contamination. In this paper, paste and mortar-based Portland cement samples with up to 70.0 wt% of steel dust were investigated. Since it is known that for one ton of Portland cement fabricated 900 kg of CO_2 are emitted to the environment, the addition of steel waste to cement is very beneficial. Moreover, since steel dust reduces the amount of needed cement in concrete, it reduces the final cost of concrete significantly. Additionally, the manufacturing processing was conducted entirely at room temperature; therefore, the negative impact of cement in the environment is reduced.

Scanning electron microscopy and X-ray diffraction characterization were conducted in order to investigate the microstructure of the samples. In addition, compression, density, and flow table tests were done over all samples. Thermo-gravimetric tests were performed to analyze the waste thermal stability. The effect of the potential hazardous components of this waste in water was analyzed through leachability tests. For all samples, compressive strength ranged from 73 to 2.5 MPa. The lowest strength value corresponded to 70 wt% of waste. Results show a solution for using this waste as admixture in cements and concrete, and therefore as a method for reducing cement paste in buildings and infrastructure.
© 2016 Elsevier Ltd. All rights reserved.

1. Introduction

The utilization of diverse forms of hazardous wastes in new materials, or recycling of them into the original components is a critical factor in the sustainability of our planet [1]. Competitive industrialization and stronger regulations are now forcing companies around the world to have zero waste. Metallurgical wastes are among those with the most negative impact on the environment by the dumping of tons of wastes per year, which contain hazardous metals and compounds [2]. Among them, steel slag is substantially concerning nowadays due to the amount generated worldwide; e.g., more than fifty million tons per year of steel slag are produced as waste material in the world [2]. Steel slag is a by-product of the conversion of iron to steel process [3]. Because of its variations in the chemical composition, its properties can vary depending on the raw materials and manufacturing process. Slag usually is classified from either the conversion process of iron to steel in a basic oxygen furnace (BOF), or the melting of scrap to fabricate steel in an electric arc furnace (EAF) [4].

Metallurgical wastes such as steel slag and dust wastes are an international issue because steel consumption is increasing around the world. Since cement and concrete are the most widespread used material of the planet, and it is well known that for a ton of cement, about 1 ton of CO_2 is released to the environment. Therefore, the use of steel slag as concrete admixture, as filler or as raw material for concrete production, represent an important beneficial manufacturing process for our environment. Taken this into the account, it has been given little attention to the use of steel slag in the production of Portland cement and concrete [5]. Therefore, more research is needed and developments that utilize different steel slag formulations.

Steel slag has been used in applications such as Portland cement [1,5], asphalt concrete [6,7], and wastewater treatment [8,9]. Few investigations using steel slag with high ZnO contents have been reported. Alsheyab and Khedaywi [10] used steel slag with 29 wt% content of ZnO in asphalt cement mixture. Further, Alsheyab [11] in another research used steel slag with 18.7 wt% in asphalt mixtures. Most researchers have used steel slag with content less

* Corresponding author at: Universidad de Antioquia, Facultad de Ingenieria, Bloque 20, Calle 67 No. 53-108, Medellin, Colombia.
E-mail address: henry.colorado@udea.edu.co (H.A. Colorado).

http://dx.doi.org/10.1016/j.conbuildmat.2016.02.201
0950-0618/© 2016 Elsevier Ltd. All rights reserved.

than 1% of ZnO in concrete [12–24]. In contrast, typical steel slag contents have been 45 wt% [24] to 80 wt% [18] in cements, and 50 wt% in concrete [12,23].

On the other hand, steel dust is a solid industrial hazardous waste generated in the collection of particulate material during the steel making process mostly referred as Electric Arc Furnace Dust (EAFD) [25], and it is classified as a hazardous waste by the Environmental Protection Agency (EPA), designated as K061 [25], because it contains hazardous metals, such as lead and Cadmium. More than 3.7 million tons per year is the estimated worldwide production of EAFD [26]. In an EAF about 15–25 kg of dust is produced per ton of steel [27]. High zinc contents appears in the waste because when galvanized steel is used in the electric arc furnace (EAF), most of the zinc is emitted as dust and fume. It is because the zinc vapor pressure is higher than iron vapor pressure [27]. Mainly, zinc is emitted as ZnO and $ZnFe_2O_4$ compounds [26]. Among few investigation of EAFD as an admixture, additive or filler for construction and building materials, ecological bricks have shown to be a promissory solution for the utilization of this waste [28].

Additionally, few studies involving leachability tests over the steel dust byproducts with cement and concrete have been conducted when superfine steel dust particles were used. Most research deal with micro and macro slag particles in cement and concrete [15–17,21]. Some studies about superfine steel slag have been reported, but those studies have been focused in the pozzolanic activity [29,30].

Although environmental regulations are becoming tougher around the world [1], many countries still do not have waste management laws over many hazardous solid wastes. In fact, many environmental regulations are only in the planning stages, as in the case of Colombia, South America, were regulations have not only limited scope, inadequate administrative support and the inexistence of effective control mechanisms and public participation [31]. In Colombia, slags are mostly unused, and particularly steel slag is only dispose in government disposal facilities. From there, this hazardous wastes could reach water sources in the worst case.

The aim of this investigation is to incorporate steel dust to White Ordinary Portland Cement (WOPC) in order to reduce the current negative impact of this waste in the environment. WOPC was used in order to qualitatively see the color changing in samples as the waste content increases, which could lead in a new set of inorganic colorants for cements. Overall, this research focused in two main goals. First, to immobilize the steel slag in concrete; thus, to reduce the risk of waters contamination. Second, to reduce the amount of cement in concrete, which can be done using this waste material as an admixture. This contributes to the reduction of the CO_2 released to the atmosphere by the utilization of less cement binder in concrete, particularly when the admixture has pozzolanic properties.

For structural applications, it is necessary to determine some optimal formulations with a compressive strength as the main criteria. From the environmental remediation point of view, it is better to incorporate as much waste as possible in the cement paste; however, a large amount no necessarily provides the maximum strength. Thus, in this research many samples were prepared with different waste loadings and water to cement (W/C) ratios. This could allow to find good formulations for structural applications and optimizing its positive impact on the environment. For planning the sampling and experiments, some of the methods applied to phosphate cements [32–34] were used, since it is common in phosphate research to used loadings up to several times those used with traditional Portland cements with wastes.

2. Experimental

White Ordinary Portland Cement (WOPC) from Holcim S.A., Colombia (with max. 6.0 wt% MgO, and max. 3.5 wt% SO_3) was used in combination with steel slag, a solid waste from Ternium Colombia. WOPC was used in order to qualitatively see the color changing in samples with the addition of slag waste. Two types of samples were investigated: cement paste with waste and cement mortar with waste.

Samples of Portland cement paste with steel slag contents were obtained first by mixing mechanically the cement powder with deionized water, and then by adding the powder waste. For some compositions, sand was added as well. In order to cover many possible compositions and Water to Cement ratios (W/C), two experiments were made: a) samples keeping constant the water content over the total amount of solid powders, and b) samples keeping constant the W/C ratio. Thus, ratios from 0.4 to 1.8 of W/C were used, and content waste from 0.0 wt% to 80 wt % over the total powders content were reached. Sample compositions for cement paste with the slag using constant W and W/C ratios are summarized in Table 1a and b respectively, for which W: water, C: cement, and SL: steel slag.

Table 2 summarizes the sample composition for the cement mortar with waste. These proportions for the mortar samples were one part of cement to one part of graded standard sand by weight and contaminant [36]. In the preparation of the mortars, the water/cement ratio (W/C) was kept constant as 0.485, and the cement was replaced by the contaminant; always keeping constant the sand-(cement + waste) ratio in 1.0. Initially, it was attempted to manufacture mortars with sand-(cement + waste) ratios of 1:2.75 at the same water-(cement + waste) ratio used for preparation of the grouting samples (0.485). However, these combinations resulted in mortars with poor fluidity to prepare mortar cubes for compressive strength tests. Then, in order to prepare the mortars keeping the same percentage of waste used in the preparation of grouting samples, it was found that sand-cement + waste) ratios of 1:1 with a constant water-(cement + waste) ratio of 0.485 resulted in good mortar fluidity (around 100%), which allowed the preparation of mortar cubes for the compression test. Also, it made consistent the water-(cement + waste) ratio for the mortar test preparation, like the water-(cement + waste) ratio used for the grouting samples. For all samples, mixing was conducted mechanically. To evaluate the effect on the contaminant on the fresh mortar, flow table tests were conducted following the ASTM C 230 standard [37].

All cement paste samples were released from molds and tested after 28 days. Compression tests were conducted in an Instron machine 3382. A set of 5 samples (diameter 20 mm × length 30 mm) was evaluated for each composition, using a crosshead speed of 1 mm/min. Modulus of elasticity was evaluated with the extensometer fixture. For cement mortar samples, immediately upon completion of

Table 1
Samples of Portland cement paste with steel dust contents: a) keeping constant W; and b) keeping constant the W/C ratio. W: water, C: cement, SD: steel dust.

a) W = Const.				b) W/C = Const.			
Sample	C (wt%)	SD (wt%)	W/C	Sample	C (wt%)	SD (wt%)	W/C
W1	100	0	0.4	W/C1	100	0	0.4
W2	99	1	0.4	W/C2	99	1	0.4
W3	97.5	2.5	0.4	W/C3	97.5	2.5	0.4
W4	95	5	0.4	W/C4	95	5	0.4
W5	90	10	0.5	W/C5	90	10	0.4
W6	80	20	0.5	W/C6	80	20	0.4
W7	60	40	0.6	W/C7	60	40	0.4
W8	50	50	0.7	W/C8	50	50	0.4
W9	40	60	0.9				
W10	30	70	1.2				

Table 2
Cement mortar with sand/(C + SD) = 1.0. W: water, C: cement, SD: steel dust.

Sand/(C + SD) = 1.0			
Sample	C (wt%)	SD (wt%)	W/C
M1	100	0	0.485
M2	99	1	0.485
M3	97.5	2.5	0.485
M4	95	5	0.485
M5	90	10	0.485
M6	80	20	0.485
M7	60	40	0.485
M8	50	50	0.485

molding, samples were kept moist within the mold during 24 h. Then, after another 24 h, samples were removed from molds, and immersed in a water tank for 28 days of curing. The compression tests over these mortar samples were conducted according to the ASTM C109 standard [38]: after the flow test, mortars were tamped by hand in the two inches molds.

Structural characterization was obtained by XRD experiments with an X'Pert PRO diffractometer (Cu Kα radiation, λ = 1.5406 Å), using 45 kV voltage and scanning between 28° and 58°. Scanning electron microscopy (SEM) was used to observe the microstructure variation of the samples. The sample preparation required that the samples were dehydrated in a furnace at 30 °C for 24 h. Next, the samples were cracked to expose the microstructure. Thereafter, they were mounted on an aluminum stub and gold sputtered with a Hummer 6.2 system, at conditions of 15 mA AC for 30 s, in order to obtain a thin film of Au of around 1 nm. The SEM used was a JEOL JSM 6700R in a high vacuum mode.

X-ray fluorescence (XRF) for oxides identification was conducted in an ARL 8680 apparatus following the ASTM C114-03 Test. Powders were dried at 105°C before the test. Loss of ignition was determined at 950 °C by thermogravimetric analysis (TGA) in a Perkin Elmer Instruments Pyris Diamond TG/DTA equipment, with a temperature ramp of 10 °C/min, and a nitrogen flux of 60 ml/min.

Density tests were conducted over all samples fabricated by simply measuring the weight and cylinders dimensions. Every composition was measured on five samples.

Additionally, at the end of the curing period, a sample of the water, which was used during the curing process, was analyzed to evaluate the leaching of heavy metals: As, Cd, Pb, and Hg. The analyses were performed based on the Standard Methods for the Examination of Water and Wastewater [39]. Regulation limits for the leaching were obtained from CFR EPA 40, Part-261.31.

3. Results

Fig. 1a shows a SEM image of the steel slag powder, where it is noticed that most of powders are below 1 µm. Therefore, due to its high surface area, those are classified like super-fine steel slag powder, which can cause more damage to environment if eventually leaching occurs. Details of the waste in big-bags while placed in El Guacal land disposal facility unit are shown in Fig. 1b and c.

Table 3 shows the steel slag composition obtained by XRF. The highest component of the slags was ZnO, with 50.48 wt%. A significant amount of Fe_2O_3 was also found, with 21.15 wt%.

Fig. 2 shows TGA results for the steel slag waste. After 1000 °C, 11 wt% is lost. At 208 °C appears a peak in both the weight derivate and heat flow curves, which corresponds to water lost of about 1.7 wt% of the total weight. At 788 °C there is a significant peak associated with the decomposition of calcium carbonate ($CaCO_3$) in calcium oxide (CaO). This decomposition occurs between 600 and 800 °C [35]. The $CaCO_3$ formation is presented in Eq. (1), while its decomposition is shown in Eq. (2). $CaCO_3$ is typically formed at the same time of the dehydroxylation of calcium hydroxide (Ca(OH)$_2$), when some of this Ca(OH) carbonated in the presence of CO_2 [35].

$$Ca(OH)_2 + CO_2 \rightarrow CaCO_3 + H_2O \tag{1}$$

$$CaCO_3 \rightarrow CaO + CO_2 \tag{2}$$

The grain size distribution of the sand used for the preparation of the mixture is shown in Fig. 3, which was prepared according to ASTM C778-13 standard specification for standard sand [36].

Typical cement paste samples fabricated after 28 days of curing in the mold are shown in Fig. 4a, while typical cement mortar samples, while cured in water are shown in Fig. 4b. After the curing process in water, samples did not show up a visual change on the surface, as presented in Fig. 4c. Fig. 5 shows a ternary phase diagram for cement paste samples. The compressive strength indication for the higher values of strength as the water and waste content is reduced, is later explained in this paper with the corresponding mechanical and microstructural characterization.

Fig. 6a shows the XRD for the samples of cement with steel slag fabricated with constant water content. The neat cement sample (cement paste with 0.0 wt% of steel slag) is itself a multiphase composite material with typical cement phases: tricalcium silicate (Ca_3SiO_5 in cement notation as C_3S), dicalcium silicate (Ca_2SiO_4 in cement notation as C_2S), cristobalite (SiO_2), mullite ($Al_6Si_2O_{13}$) and tetracalcium aluminoferrite (Ca_2AlFeO_5 in cement notation as C_4AF). Adding steel slag to the neat cement paste produces new phases: Sphalerite (ZnS), manganese oxide (Mn_3O_4), zincite (ZnO), and Magnesioferrite ($MgFe_2O_4$). As a general trend, it is observed that as the cement amount decreases (waste increases), the intensitive of these phases decreases as well. This trend is also observed in Fig. 6b, which shows the XDR for cement-steel slag samples keeping constant the W/C ratio. It is also observed that as waste content increases, the sample gets a more crystalline material, which is associated to the presence of both unreacted steel dust and new forming phases. At 36° appear peaks from Fe_2O_3 and ZnO because the high amount of unreacted waste, but also appears a strong peak of $MgFe_2O_4$, clearly formed as a new

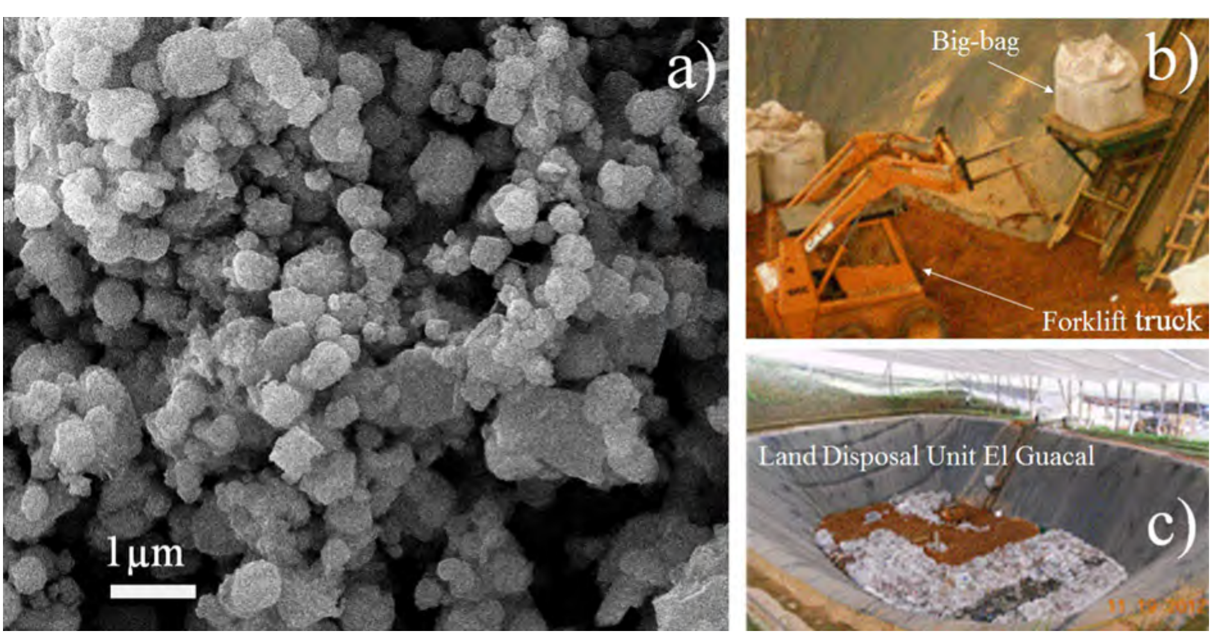

Fig. 1. a) Steel dust powder, b) big-bags location in the land disposal unit El Guacal, c) site overview.

Table 3
XRF results over the steel dust, with loss of ignition of 11%.

Oxide	ZnO	Fe_2O_3	Na_2O	MgO	Mn_3O_4	SiO_2	SO_3	K_2O	CaO	Al_2O_3	SrO
wt%	50.40	21.54	3.38	2.55	2.43	2.12	1.90	1.32	1.20	0.77	0.004
Oxide	BaO	Cr_2O_3	P_2O_5	CuO	HfO_2	TiO_2	PbO	NiO	V_2O_5	ZrO_2	LOI
wt%	0.472	0.26	0.172	0.19	0.115	0.035	0.025	0.020	0.006	0.001	11

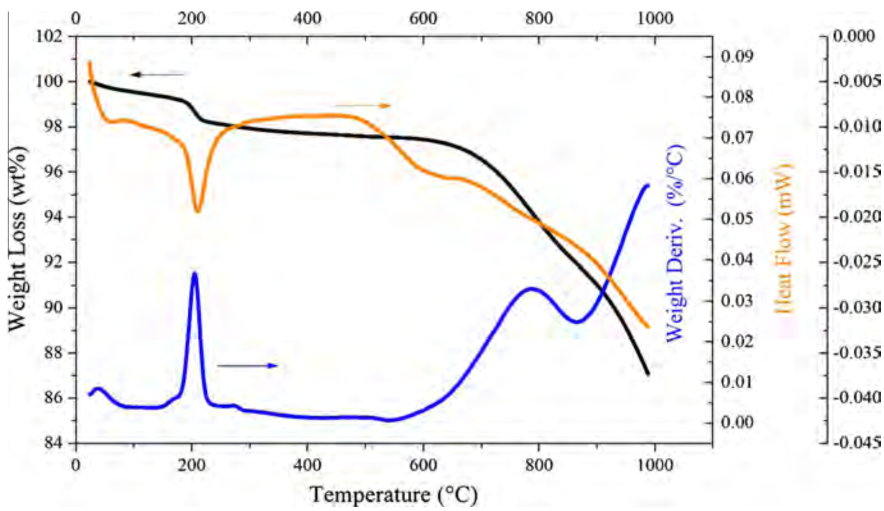

Fig. 2. TGA results for the steel dust waste.

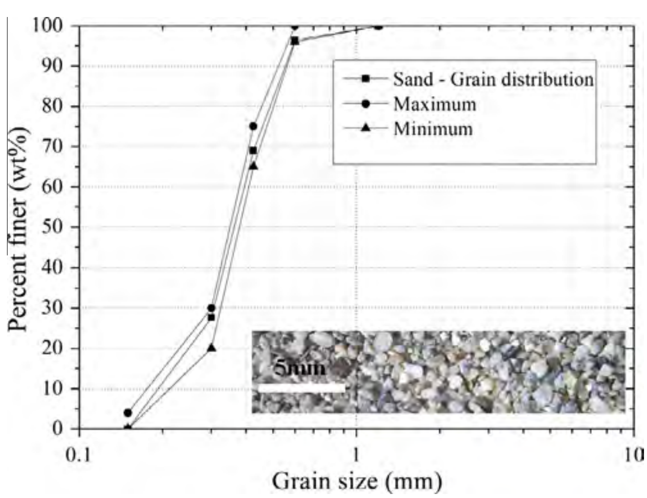

Fig. 3. Grain size distribution of the sand used for the mortar.

phase when compared with the neat cement paste. $MgFe_2O_4$ is spinel ferrite with interesting magnetic and electrical properties as reported before [40]. $MgFe_2O_4$ is classified as a soft magnetic *n*-type semiconducting material used in several applications including heterogeneous catalysis, adsorption, sensors, and magnetic technologies [40]. The formation of this magnetic phase in the cement paste could lead in new cementitious materials and composites with enhanced magnetic properties upon the optimization of the amount of this phase coming from an abundant steel dust source worldwide.

Fig. 7 is a summary of selected SEM images from all samples. Fig. 7a corresponds to the neat cement paste sample showing primarily calcium silicate hydrate (C-S-H). As steel slag contents was increased, a less continuos structure resulted, which is due to a high amount of slag with poor impregnation of the cementitious matrix. Fig. 7b also shows C-S-H, but some micro particles of steel slag appeared. As the waste loading was increased (such as in Fig. 7c, d and e) more waste is visible, and the fracture mode also changed to a more smooth fracture surface. Fig. 7f corresponds to samples with 50 wt% of waste with W/C = 0.4, which are similar in the microstructure (highly loaded) and the failure mode to Fig. 7d.

Fig. 8a shows the compressive strength values for fabricated samples, keeping constant W and W/C. Results show that the strength of the samples is reduced as the waste content is increased. Strength value for samples with 80 wt% waste content for W/C constant is not shown because under the sample condition of W/C constant it was not possible to consolidate good solid samples; therefore, there were not samples for this tests. Samples were very weak at the point, and it was not possible to release them from the mold without damage.

Thus, the lowest strength value for samples tested in this research, corresponding to 70 wt% of waste, showed a mean value of 7.1 MPa, which is good enough for decoration, waste stabilization and other non-critical structural applications.

Fig. 8b shows the density tests results for the same samples tested in compression. In general, samples with water content constant had higher density values. This is explained checking Table 1a and b, in which samples with W constant had in general higher water contents for the same waste amount than sample with W/C constant. The higher water contents decreases the viscosity of the mix and increases its wettability over the steel slag particles.

Compressive strength for mortar samples is shown in Fig. 9a. Results showed that as waste content increased, the compressive strength decreased. For waste less than 20 wt%, the strength decrease is acceptable, but for bigger waste contents the strength lost is very significant.

Fig. 9b shows moduli results for the mortar cement type sample, where is clearly noticed that as waste content increases, the moduli decreases. This is an expected result since at very high

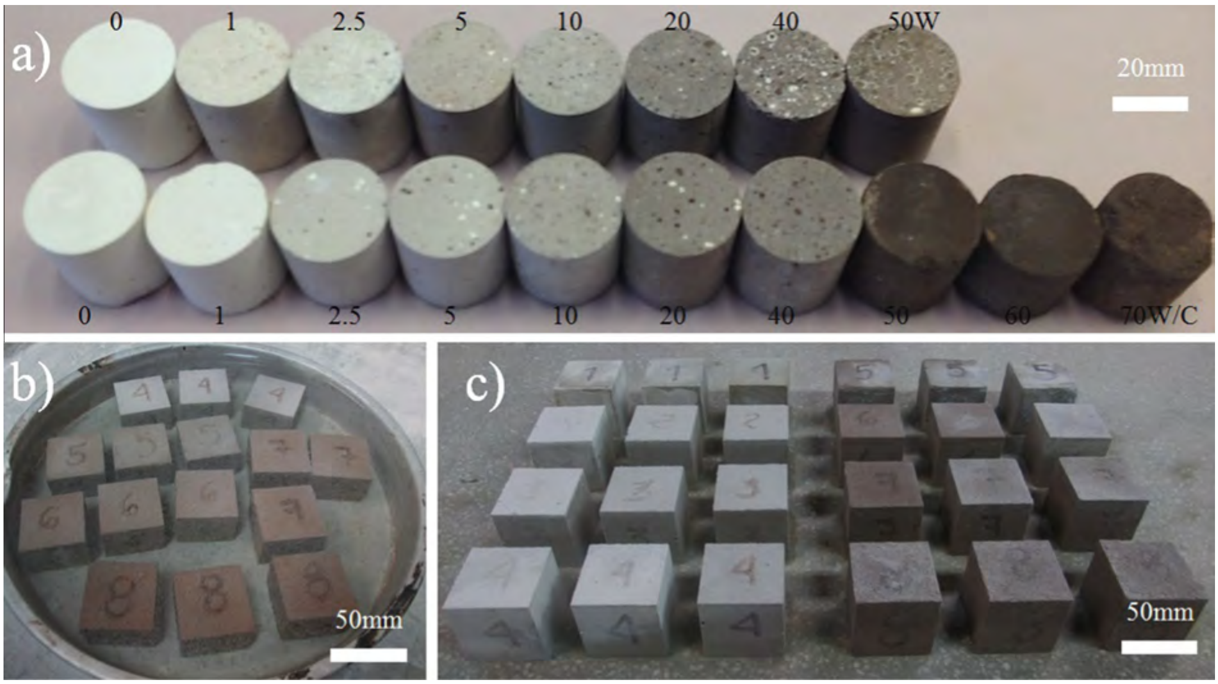

Fig. 4. Typical samples fabricated, a) cement paste with steel dust; b) cement mortar samples being cured in water, c) cement mortar samples just before compression tests.

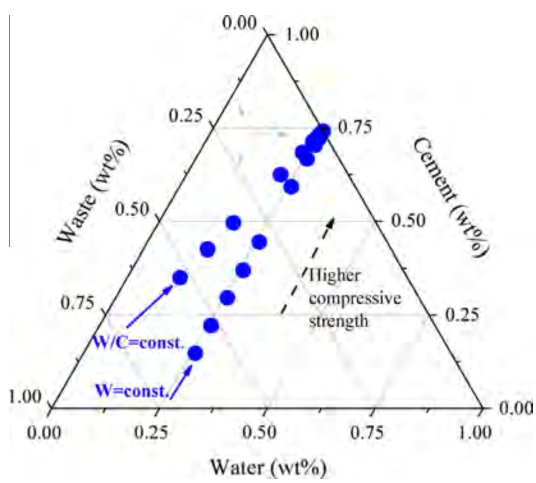

Fig. 5. Ternary phase diagram for samples fabricated while keeping constant water to cement ratio (W/C) or water (W) contents.

waste content the compressive strength is reduced and agglomeration of the waste increases due to a reduction in the bonding materials content. The maximum value was obtained for the sample with 1.0 wt% of waste, which is consistent with the compressive strength. These results were observed for compression and density tests in both the paste and the mortar samples.

The relationship between the percentage of contaminant within the mortar and the mortar flow value is presented in Fig. 9c. From this figure, it is seen a trend of reduction of the flow value for the mortar with a contaminant content less than 10%. The minimal value of flow is attained for the mortar with a content of 10% of contaminant; for contents larger than 10% of the contaminant mixture, the flow values increased linearly.

Finally, leachability results are summarized in Table 4. They showed that the typical hazardous elements of this waste, such as As, Cd, Pb, and Hg are far below the regulation limits [41]. This is a very significant result since this waste is classified in the world as hazardous for having some of these materials over the maximum allowed by law. Notice that this water contained a combination of leaching results for samples with different compositions. Moreover, samples with up to 50 wt% of slag are included there (M8 samples from Table 2). This means that low concentration of slag is even more safe, and cement is more efficient to stabilize the waste.

4. Discussion

The amount of steel slag and steel dust produced worldwide is enormous. Just for stainless steel industry, the stainless steel production in the first half of 2012 [42] was estimated in 17.2 Mt (about 34 Mt/y). Estimations suggest that the slag/steel ratio is around 0.33 (t_{slag}/t_{steel}) [43], therefore, the steel slag is about 11 Mt/y. On the other hand, cement production approaches to 4000 Mt/y [44], which could mean that up to 3600 Mt/y of CO_2 emitted to the air (for about one ton of Portland cement fabricated 900 kg of CO_2 are emitted to the environment). Thus, the reduction in cement paste by adding steel slag is beneficial for both environment and product cost. Moreover, the slag itself can have hazardous metals, so cement paste acts as a waste stabilizer. All these advantages were confirmed in this paper. These huge production justify any of our results because of the need we have to find multiple application for the diverse waste compositions: even for the lowest compressive strength values, corresponding to the highest loadings of waste, compressive strength enables the mix to be used in decoration or similar non high strength applications.

In addition, the relation of Strength/Density (S/D) was analyzed and showed a similar trend than individual strength and density curves. S/D was reduced up to 49% and 30% (with respect samples with 0.0 wt% of waste) for samples with W/C constant and W constant respectively. The highest S/D reduction was about 12% for the 70 wt% of waste, which could be improved via admixtures and reinforcements in a future research.

Almost no research is found for steel dust with high concentration of ZnO and for micro size powders as an admixture for cement, both investigated in this research. In Colombia and many countries

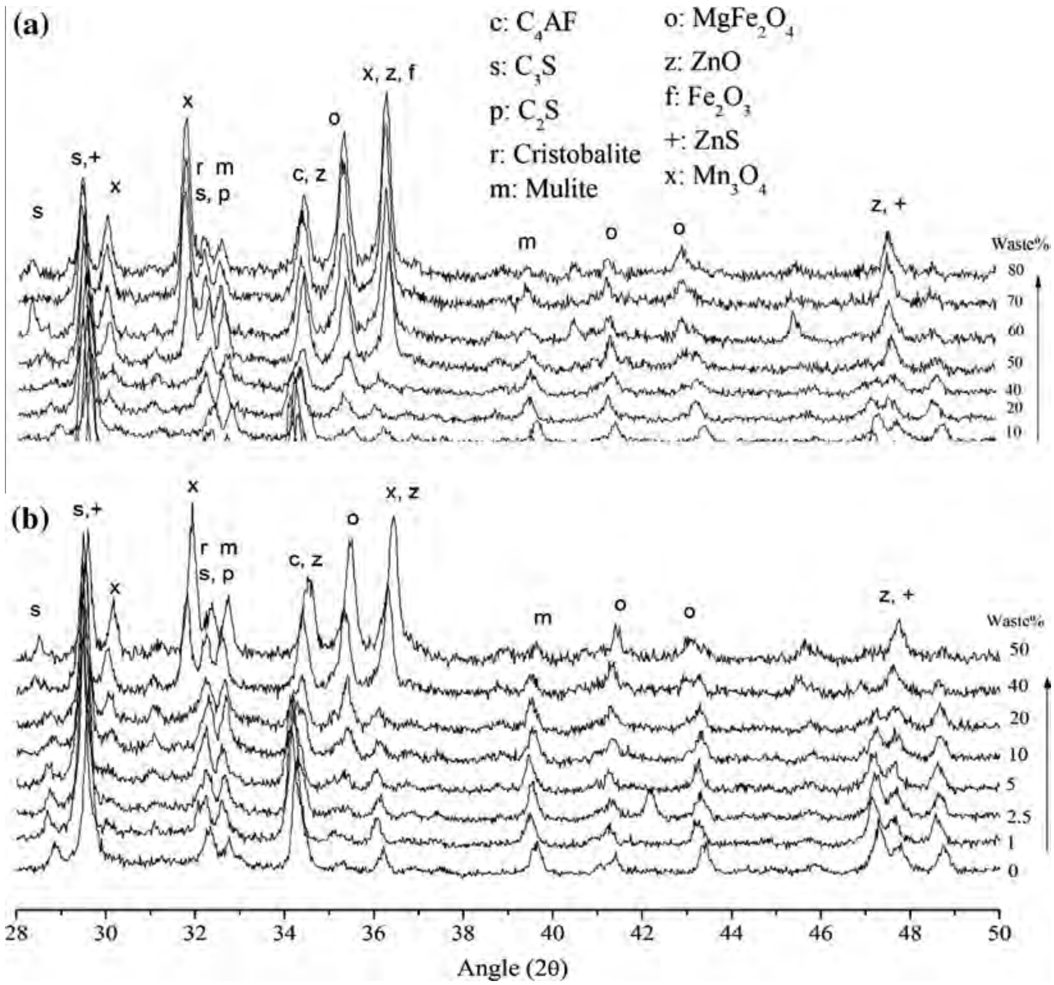

Fig. 6. XRD data for the cement-steel dust composite samples, keeping: a) constant water, b) constant W/C ratio.

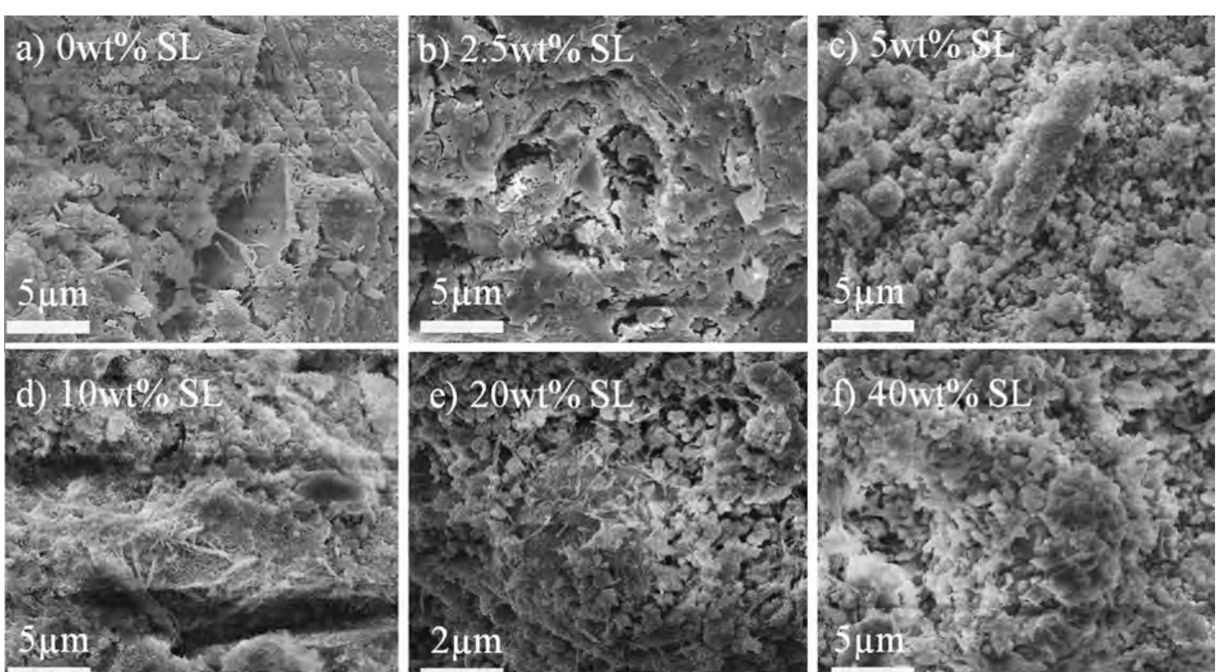

Fig. 7. SEM images for the cement-steel dust composites. All samples have W/C = 0.4.

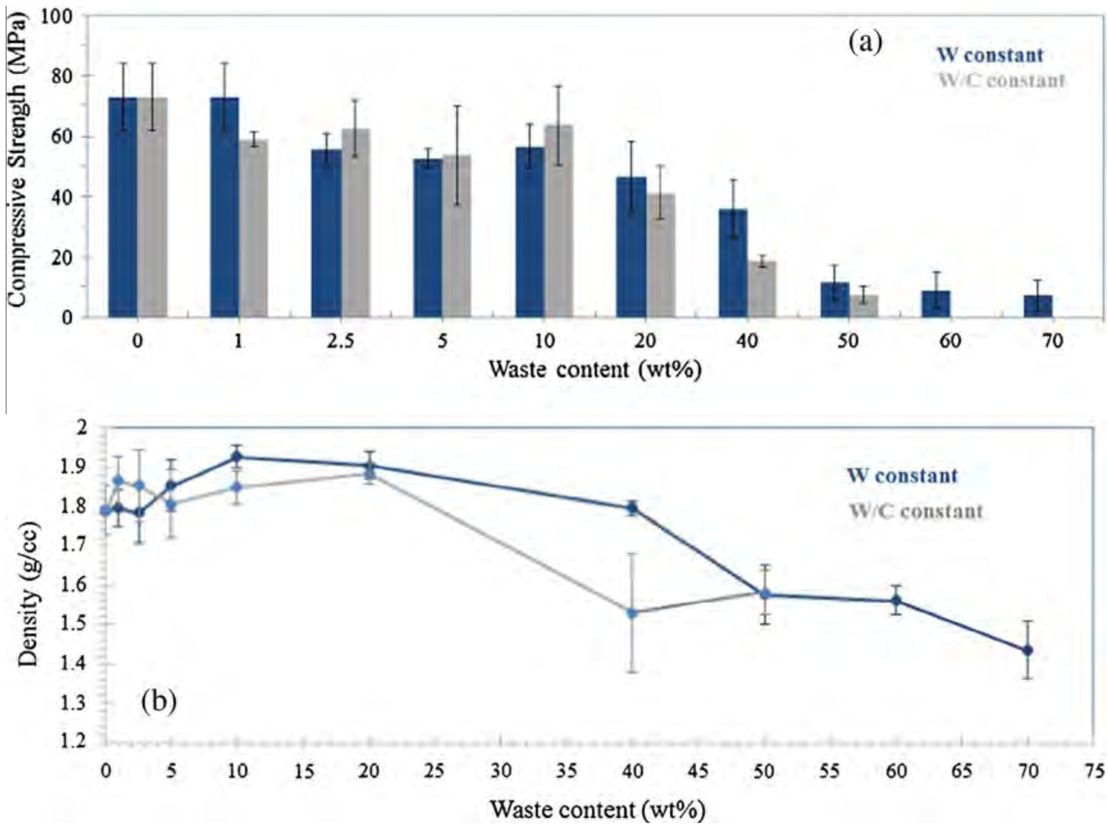

Fig. 8. a) Compressive strength for the cement-steel dust composites fabricated, b) density results for same samples from a).

worldwide, all types of steel slags are only disposed underground in government disposal facilities, which by leaching can release hazardous components to groundwater, rivers, and lakes. The leachability results obtained from the water used to cure mortar samples revealed that all these elements were under the detection limits. This is very significant considering that the water tested had all samples at the same time, and some of them had 50 wt% of waste. Further improvement of the waste stability in water could lead to formulations with high thermochemical stability and high waste loadings. On the other hand, the slag used had two special conditions: it is superfine, and it has a very high ZnO concentration. These characteristics and overall results suggest the possibility to have in the near future cementitious materials with tailored piezo-electric properties.

It has been reported [5] that one of the main issues with steel slag in infrastructure is the possible presence of free lime: when the slag is hydrated, its volume increases, and therefore the corresponding swelling in large-sized components can cause major damages. However, in our investigation for steel dust when samples were cured in water, no damage or second phase formation was observed. ZnO addition to cement mix with water generally agreed to retard hydration [47], and since our waste has 50.4 wt % of ZnO, we should expect a longer setting time. Preliminary observations in this research showed not significant changes in the setting time, which suggest a complex role of all oxide mix composing the steel dust, see Table 3. It was observed that as waste increased the cement setting need it more time to get harder. Although all cement paste samples were released after 28 days of curing, those samples with more than 50 wt% of steel dust were hard to release from molds because they looked very weak. This is an expected result as is well known that ZnO and Zn ions are retardants of cement hydration. ZnO contents as low as 0.5 wt% can increase by 5 times the setting of cement [45,46]. Adversely, Fe_2O_3 is used in the fabrication of Portland cement as constituent of several phases, but its effects on the hydration process is poorly understood, although there is some information reporting to have a poor or not effect on the setting time [48]. Since we have 21.5 wt % of this material in the slag, we assumed that the retarding effect on hydration by ZnO is being cancelled by other oxides in minor contents. Due to the complex composition of slags, it is reported that the effect of the slag on the hydration is still not completely understood [49].

The compressive strength of both cement paste and mortar samples in general decreased with the waste content. The highest value for cement past samples was obtained for 1.0 wt% of waste, which make sense since some of the slag particles are too small that could participated as void filler. In the cement mortar samples strength always decreases with the waste content as well (highest strength was for 0.0 wt% of slag), which could improve upon the optimization of both the mixing process and the selection of better aggregate particle size. Considering the amount of CO_2 released during the Portland cement manufacturing, this investigation showed that even high loadings of steel dust (with high concentration of ZnO) have acceptable structural properties. This result lead into cements with less amount of the traditional cementing material, which can be replaced by a proper waste.

As shown in the TGA experiment, the thermal stability of this waste is good enough (at 800 °C only lost about 6 wt% of mass) for typical concrete applications involving infrastructure or waste stabilization. Samples fabricated are stable in water at room temperature conditions, which could open up new applications for cement and concrete with superfine steel dust. Further experiments are needed in order to evaluate the cement paste-steel dust mixture for formulations targeting high temperature applications, and ZnO and other particle functionalization in order to optimize the matrix-particle interaction [50].

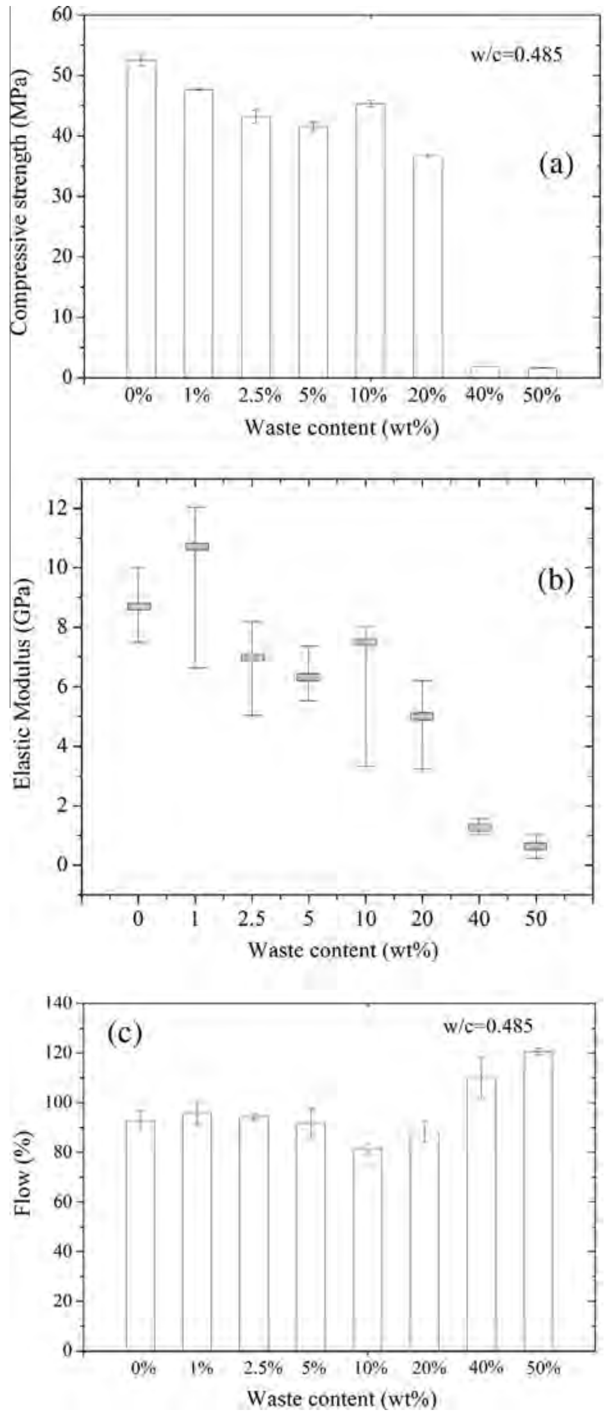

Fig. 9. Results for cement mortar samples: a) compressive strength, b) elastic modulus, c) flow table test.

Table 4
Leaching tests results over the water used for curing the mortar samples

Element	Units	Detection limit (DL)	Regulation	Reference water	Leachate
As	mg/L	0.00042	5.0	<DL	0.0118 ± 0.001
Cd	mg/L	0.001	1.0	<DL	<DL
Pb	mg/L	0.010	5.0	<DL	0.262
Hg	mg/L	0.00014	0.2	<DL	<DL

5. Conclusion

Portland cement-steel dust waste composites were fabricated in this research. Up to 80 wt% over the total amount of powders were added and mixed mechanically. The lowest compressive strength found was 7.1 MPa corresponding to the sample with 70 wt% of steel dust. Even this value is competitive for many applications involving infrastructure and building materials such as decorative and other non structural parts. Results shows adding this slag to cement reduces the negative effect of slag in environment and reduces the cement binding in cement- and concrete-based products.

Considering the data of CO_2 produced by the fabricated Portland cement, samples fabricated in this research are up to 70.0 wt% of steel dust, which can reduce up to 630 kg of CO_2 emitted to air per ton of fabricated cement. Moreover, since this steel waste reduces the amount of cement needed in concrete, it reduces the final cost of concrete significantly.

Although it is clear that samples with less waste had better strength, due to the complex multiphase materials found in the sample, it is necessary to conduct more research particularly in the hydration mechanisms. Leaching results over the water used for curing tests showed hazardous materials were all below the maximum permitted limits.

Acknowledgements

The authors wish to thank to Mr A. Norena for supplying the waste materials.

References

[1] D. Griggs, M. Stafford-Smith, O. Gaffney, J. Rockström, M.C. Öhman, P. Shyamsundar, W. Steffen, G. Glaser, N. Kanie, I. Noble, Policy: sustainable development goals for people and planet, Nature 495 (7441) (2013) 305–307.
[2] I.A. Altun, I. Yılmaz, Study on steel furnace slags with high MgO as additive in Portland cement, Cem. Concr. Res. 32 (8) (2002) 1247–1249.
[3] I.Z. Yildirim, M. Prezzi, Chemical, mineralogical, and morphological properties of steel slag, Adv. Civ. Eng. 2011 (2011).
[4] J. Li, Q. Yu, J. Wei, T. Zhang, Structural characteristics and hydration kinetics of modified steel slag, Cem. Concr. Res. 41 (3) (2011) 324–329.
[5] P.E. Tsakiridis, G.D. Papadimitriou, S. Tsivilis, C. Koroneos, Utilization of steel slag for Portland cement clinker production, J. Hazard. Mater. 152 (2) (2008) 805–811.
[6] S. Wu, Y. Xue, Q. Ye, Y. Chen, Utilization of steel slag as aggregates for stone mastic asphalt (SMA) mixtures, Build. Environ. 42 (7) (2007) 2580–2585.
[7] P. Ahmedzade, B. Sengoz, Evaluation of steel slag coarse aggregate in hot mix asphalt concrete, J. Hazard. Mater. 165 (1) (2009) 300–305.
[8] J. Xiong, Z. He, Q. Mahmood, D. Liu, X. Yang, E. Islam, Phosphate removal from solution using steel slag through magnetic separation, J. Hazard. Mater. 152 (1) (2008) 211–215.
[9] A. Drizo, C. Forget, R.P. Chapuis, Y. Comeau, Phosphorus removal by electric arc furnace steel slag and serpentinite, Water Res. 40 (8) (2006) 1547–1554.
[10] M.A.T. Alsheyab, T.S. Khedaywi, Effect of electric arc furnace dust (EAFD) on properties of asphalt cement mixture, Resour. Conserv. Recycl. 70 (2013) 38–43.
[11] M.A.T. Alsheyab, SEM analysis on electron arc furnace dust (EAFD) and EAFD-asphalt mixture, Environ. Nat. Resour. Res. 3 (4) (2013) p147.
[12] H. Qasrawi, F. Shalabi, I. Asi, Use of low CaO unprocessed steel slag in concrete as fine aggregate, Constr. Build. Mater. 23 (2) (2009) 1118–1125.
[13] H. Yi, G. Xu, H. Cheng, J. Wang, Y. Wan, H. Chen, An overview of utilization of steel slag, Proc. Environ. Sci. 16 (2012) 791–801.
[14] J.L. Calmon, F.A. Tristão, M. Giacometti, M. Meneguelli, M. Moratti, J.E.S.L. Teixeira, Effects of BOF steel slag and other cementitious materials on the rheological properties of self-compacting cement pastes, Constr. Build. Mater. 40 (2013) 1046–1053.
[15] J.T. San-José, I. Vegas, I. Arribas, I. Marcos, The performance of steel-making slag concretes in the hardened state, Mater. Des. 60 (2014) 612–619.
[16] A.S. Brand, J.R. Roesler, Steel furnace slag aggregate expansion and hardened concrete properties, Cem. Concr. Compos. 60 (2015) 1–9.
[17] I. Arribas, A. Santamaría, E. Ruiz, V. Ortega-López, J.M. Manso, Electric arc furnace slag and its use in hydraulic concrete, Constr. Build. Mater. 90 (2015) 68–79.
[18] R. Siddique, R. Bennacer, Use of iron and steel industry by-product (GGBS) in cement paste and mortar, Resour. Conserv. Recycl. 69 (2012) 29–34.

[19] Y.N. Sheen, H.Y. Wang, T.H. Sun, Properties of green concrete containing stainless steel oxidizing slag resource materials, Constr. Build. Mater. 50 (2014) 22–27.
[20] H. Qasrawi, The use of steel slag aggregate to enhance the mechanical properties of recycled aggregate concrete and retain the environment, Constr. Build. Mater. 54 (2014) 298–304.
[21] B. Pang, Z. Zhou, H. Xu, Utilization of carbonated and granulated steel slag aggregate in concrete, Constr. Build. Mater. 84 (2015) 454–467.
[22] Q. Wang, P. Yan, J. Yang, B. Zhang, Influence of steel slag on mechanical properties and durability of concrete, Constr. Build. Mater. 47 (2013) 1414–1420.
[23] V.S. Devi, B.K. Gnanavel, Properties of concrete manufactured using steel slag, Proc. Eng. 97 (2014) 95–104.
[24] S. Kourounis, S. Tsivilis, P.E. Tsakiridis, G.D. Papadimitriou, Z. Tsibouki, Properties and hydration of blended cements with steelmaking slag, Cem. Concr. Res. 37 (6) (2007) 815–822.
[25] K061, Emission Control Dust/Sludge from Production of Steel in Electric Furnaces, United States Environmental Protection Agency, 1983 (July 11).
[26] J.G. Machado, F.A. Brehm, C.A.M. Moraes, C.A. Dos Santos, A.C.F. Vilela, J.B.M. Da Cunha, Chemical, physical, structural and morphological characterization of the electric arc furnace dust, J. Hazard. Mater. 136 (3) (2006) 953–960.
[27] A.G. Guézennec, J.C. Huber, F. Patisson, P. Sessiecq, J.P. Birat, D. Ablitzer, Dust formation in electric arc furnace: birth of the particles, Powder Technol. 157 (1) (2005) 2–11.
[28] E.A. Dominguez, R. Ullman, 'Ecological bricks' made with clays and steel dust pollutants, Appl. Clay Sci. 11 (2) (1996) 237–249.
[29] Y. Shi, H. Chen, J. Wang, Q. Feng, Preliminary investigation on the pozzolanic activity of superfine steel slag, Constr. Build. Mater. 82 (2015) 227–234.
[30] Q. Wang, J. Yang, P. Yan, Cementitious properties of super-fine steel slag, Powder Technol. 245 (2013) 35–39.
[31] J. Toro, I. Requena, M. Zamorano, Environmental impact assessment in Colombia: critical analysis and proposals for improvement, Environ. Impact Assess. Rev. 30 (4) (2010) 247–261.
[32] H.A. Colorado, D. Singh, High-sodium waste streams stabilized with inorganic acid–base phosphate ceramics fabricated at room temperature, Ceram. Int. 40 (7) (2014) 10621–10631.
[33] H.A. Colorado, H.T. Hahn, C. Hiel, Pultruded glass fiber-and pultruded carbon fiber-reinforced chemically bonded phosphate ceramics, J. Compos. Mater. 0021998311401090 (2011).
[34] H.A. Colorado, Z. Wang, J.M. Yang, Inorganic phosphate cement fabricated with wollastonite, barium titanate, and phosphoric acid, Cem. Concr. Compos. 62 (2015) 13–21.
[35] N.H. Roslan, M. Ismail, Z. Abdul-Majid, S. Ghoreishiamiri, B. Muhammad, Performance of steel slag and steel sludge in concrete, Constr. Build. Mater. 104 (2016) 16–24.
[36] ASTM C778-13: Standard specification for standard sand, 2013.
[37] ASTM C230/CM230M-14: Standard specification for flow table for use in tests of hydraulic cement, 2014.
[38] ASTM C109/C109M-13: Standard test method for compressive strength of hydraulic cement mortars (Using 2-in. or 50-mm Cube Specimens), 2013.
[39] E.W. Rice, L. Bridgewater, Standard Methods for the Examination of Water and Wastewater, 22 ed., American Public Health Association, Washington DC, 2012.
[40] S. Maensiri, M. Sangmanee, A. Wiengmoon, Magnesium ferrite (MgFe2O4) nanostructures fabricated by electrospinning, Nanoscale Res. Lett. 4 (3) (2009) 221–228.
[41] U.S. Environmental Protection Agency (EPA), 40 CFR, Part 261.31, 1993.
[42] R.I. Iacobescu, G.N. Angelopoulos, P.T. Jones, B. Blanpain, Y. Pontikes, Ladle metallurgy stainless steel slag as a raw material in Ordinary Portland Cement production: a possibility for industrial symbiosis, J. Cleaner Prod. 112 (2016) 872–881.
[43] International Stainless Steel Forum, www.worldstainless.org/news/show/440, 2012, (accessed July 2015).
[44] U.S. Geology Survey, Mineral Commodity Summaries: Cements, 2013 (38–39).
[45] F.F. Ataie, M.C. Juenger, S.C. Taylor-Lange, K.A. Riding, Comparison of the retarding mechanisms of zinc oxide and sucrose on cement hydration and interactions with supplementary cementitious materials, Cem. Concr. Res. 72 (2015) 128–136.
[46] M.A. Trezza, Hydration study of ordinary Portland cement in the presence of zinc ions, Mater. Res. 10 (4) (2007) 331–334.
[47] H. Bolio-Arceo, F.P. Glasser, Zinc oxide in Portland cement. Part II: hydration, strength gain and hydrate mineralogy, Adv. Cem. Res. 12 (4) (2000) 173–179.
[48] M.S. Amin, S.M.A. El-Gamal, F.S. Hashem, Effect of addition of nano-magnetite on the hydration characteristics of hardened Portland cement and high slag cement pastes, J. Therm. Anal. Calorim. 112 (3) (2013) 1253–1259.
[49] E. Gruyaert, N. Robeyst, B.N. De, Study of the hydration of Portland cement blended with blast-furnace slag by calorimetry and thermogravimetry, J. Therm. Anal. Calorim. 102 (3) (2010) 941–951.
[50] Z. Guo, S. Wei, B. Shedd, R. Scaffaro, T. Pereira, H.T. Hahn, Particle surface engineering effect on the mechanical, optical and photoluminescent properties of ZnO/vinyl-ester resin nanocomposites, J. Mater. Chem. 17 (8) (2007) 806–813.